



ELSEVIER

Contents lists available at ScienceDirect

Applied Surface Science

journal homepage: www.elsevier.com/locate/apsusc

Full length article

Surface functionalization of the terraced surface-based current collector for a supercapacitor with an improved energy storage performance

Geon-Hyoung An^a, SeungNam Cha^c, Hyo-Jin Ahn^{a,b,*}^a Program of Materials Science & Engineering, Convergence Institute of Biomedical Engineering and Biomaterials, Seoul National University of Science and Technology, Seoul 01811, Republic of Korea^b Department of Materials Science and Engineering, Seoul National University of Science and Technology, Seoul 139-743, Republic of Korea^c Department of Engineering Science, University of Oxford, Parks Road, Oxford OX1 3PJ, United Kingdom

ARTICLE INFO

Keywords:

Interface engineering
Supercapacitor
Current collector
Terraced surface
Charge transfer

ABSTRACT

Due to its high electrical conductivity and excellent chemical/physical durability, the nickel (Ni) foam is conventionally used as the current collector of supercapacitors that are characterised by high power density, rapid charge/discharge cycles, and long lifespan. However, the limitation of the current collector is its flat surface, which leads to a low rate performance and cycling stability. Therefore, a rational design of the current collector and the electrode material is an essential interfacial engineering technology to be developed to improve the electrochemical performance of the collector. In the present study, applying the surface functionalization of the Ni current collector with the nano-sized stairs of the terraced surface resulted in the electrochemical performance of a remarkable capacitance (210 F g^{-1} at the current density of 0.5 A g^{-1}), excellent rate performance of 83%, and outstanding cycling stability of 89% after 10,000 cycles. The proposed design has obvious advantages in terms of the high contact area between the current collector and electrode material, on the one hand, and the uneven surface, on the other hand, leading to an excellent rate performance and an outstanding cycling stability. This remarkable capability demonstrates that the surface functionalization of the current collector is a promising technology for high-performance supercapacitors.

1. Introduction

In recent years, the wide use of electronic portable devices and electric transportations has led to an unprecedented interest in the development of environmentally-friendly, safe, and effective energy storage technologies [1–5]. In this context, due to their high-power density, rapid charge/discharge cycles, long cycle life, eco-friendliness, and safe operation, supercapacitors have become increasingly attractive as efficient energy storage devices [5–14]. Another advantage of supercapacitors is that they can give supplementary energy of fuel cells and batteries so as to provide back-up power to save against potential power disruptions. Supercapacitors have four major components: current collectors, electrodes, separators, and electrolytes.

Among the components of supercapacitors, there are two major interfaces that determine their energy storage performance: the electrode material/electrolyte and the current collector/electrode material [15,16]. Therefore, interface engineering is essential to enhance the electrochemical performance of supercapacitors. Thus far, most studies

have mainly sought to improve the electrode material/electrolyte interface using advanced nanomaterials for the electrode, which can develop the high electroactive sites and thus lead to an improvement of ionic diffusion [17–34]. However, to further enhance the energy storage performance of supercapacitors, applying interface engineering to the interface between the current collector and the electrode material is equally important. The typical material of current collectors is nickel (Ni) foam, which has several important advantages, such as its high electrical conductivity ($1.46 \times 10^7 \text{ S m}^{-1}$) and excellent chemical and physical durability [18,20,22]. Ironically, the surface development of the Ni foam as the current collector is limited owing to its superb chemical and physical stability. Therefore, the studies that sought to apply interface engineering to the current collector/electrode material interface are by far outnumbered by those focusing on the electrode material/electrolyte interface.

To fill this gap in the literature, in the present study, we propose a novel interface engineering of the Ni foam as the current collector. The electrochemical etching process was performed to obtain the surface

* Corresponding author at: Department of Materials Science and Engineering, Seoul National University of Science and Technology, Seoul 139-743, Republic of Korea.

E-mail address: hjahn@seoultech.ac.kr (H.-J. Ahn).

<https://doi.org/10.1016/j.apsusc.2019.01.280>

Received 2 May 2018; Received in revised form 26 December 2018; Accepted 29 January 2019

Available online 30 January 2019

0169-4332/ © 2019 Elsevier B.V. All rights reserved.

functionalization of the Ni foam. To promote a favourable charge transfer capability, the key technology used in the proposed approach is the high interface sites between the current collector and the electrode material.

2. Experimental

2.1. Synthesis of the surface functionalised Ni (SFNi) as current collector

The surface functionalised Ni (SFNi) as the current collector was successfully fabricated using the electrochemical etching process. The electrochemical etching process was prepared in 0.2 M hydrochloric acid solution at the 1.2 V by a potentiostat/galvanostat (Ecochemie Autolab PGST302N, Netherlands). In order to acquire the optimization performance of supercapacitors, the electrochemical etching process was gradually performed using different times (100, 150, and 200 s), referred thereafter as SFNi-100, SFNi-150, and SFNi-200, respectively. For comparison, the conventional Ni foam as the current collector (thereafter referred to as SFNi-0) was also prepared without the electrochemical etching process for comparison.

2.2. Characterization

The structures and morphologies of the SFNi-0, SFNi-100, SFNi-150, and SFNi-200 electrodes were investigated using scanning electron microscopy (SEM). The crystal structures and chemical bonding states were examined using X-ray diffraction (XRD) with Cu K α radiation and X-ray photoelectron spectroscopy (XPS) with an Al K α X-ray source, respectively.

2.3. Electrochemical characterization

Electrochemical measurements were performed using the conventional two-electrode system. The electrode slurries were prepared using the activated carbon, ketjen black, and polyvinylidene difluoride at the ratio of 8:1:1 in *N*-methyl-2-pyrrolidone coated on the SFNi-0, SFNi-100, SFNi-150, and SFNi-200 electrodes with 1 * 1 cm². The resultant electrodes were dried in air at 80 °C for 12 h. The 6 M potassium hydroxide (KOH) solution was used as the electrolyte. Electrochemical impedance spectroscopy (EIS) measurements were made at frequencies ranging from 10⁵ to 10⁻² Hz using applying an AC signal of 5 mV. Cyclic voltammetry (CV) measurements were analysed using a potentiostat/galvanostat at the scan rate of 30 mV s⁻¹ in the potential range of 0.0–1.0 V. The charging/discharging measurements were tested at the current density of 0.5–20 A g⁻¹ in the potential range of 0.0–1.0 V. The long cycling stability was measured at the current density of 5 A g⁻¹ up to 10,000 cycles.

3. Results and discussion

As illustrated in Fig. 1, the novel surface functionalization of SFNi was fabricated using the electrochemical etching process. The Ni foam was applied by 1.2 V in the electrolyte (see Fig. 1a). Thereafter, the Ni foam was etched through the dissolution of Ni²⁺ (see Fig. 1b). Finally, the surface functionalization of Ni foam with the uneven surface was successfully accomplished (see Fig. 1c). In addition, to optimise the surface functionalization of SFNi, the electrochemical etching process was gradually prepared using different times (100, 150, and 200 s).

Fig. 2 shows low-resolution (a–d) and high-resolution (e–h) SEM images of the SFNi-0, SFNi-100, SFNi-150, and SFNi-200 electrodes. All samples exhibited foam structures, indicating that the electrochemical etching process could only influence the surface morphologies. SFNi-0 (see Fig. 2a and e) showed the flat surface, signifying an inefficient utilization of the surface. On the other hand, SFNi-100 (Fig. 2b and f) presented a slightly uneven surface due to the dissolution of Ni²⁺ by the electrochemical etching process. Furthermore, SFNi-150 (Fig. 2c

and g) had a novel architecture for the nano-sized stairs of the terraced surface. Hence, it can be expected that, owing to the high contact area and the strong interfacial adhesion between the current collector and active materials, nano-sized stairs of the terraced surface as current collectors would significantly improve the electrochemical behaviour during cycling. However, SFNi-200 (Fig. 2d and h) showed a relatively flat surface without nano-sized stairs on the surface, indicating that nano-sized stairs were repeatedly etched for long times of 200 s. Thus, the electrochemical etching process was optimised at 1.2 V for 150 s, which means that the dissolution of Ni²⁺ is a promising candidate for the surface functionalization of the Ni foam.

As concerns the crystal structure, Fig. 3a shows the XRD data of the SFNi-0, SFNi-100, SFNi-150, and SFNi-200 electrodes. The main diffraction peaks of SFNi are observed at 44.5°, and 51.8°, corresponding to the (111) and (200) planes of the face-centred metallic Ni phases, respectively. Specifically, the (111) plane of Ni is more majority than the (200) plane. The crystal structures of SFNi-100, SFNi-150, and SFNi-200 were still maintained after the electrochemical etching process, implying etching of both (111) and (200) planes by the electrochemical etching process. Taken together, these results suggest that the formation mechanism for nano-sized stairs of the terraced surface would be the etching of the (111) plane of the face-centred structure induced by the dissolution of Ni²⁺. This etching process can be ascribed to the higher elastic strain energy of (111) plane of the face-centred structure, resulting in many flaws per unit area [35–37]. In order to verify the chemical binding states of the SFNi-0, SFNi-100, SFNi-150, and SFNi-200 electrodes, the XPS spectra were obtained (see Fig. 3b). The C1s (248.5 eV) was used as the reference on all signals. The XPS signals of Ni 2p were monitored at 852.2 eV, 855.0 eV, and 862.3 eV, corresponding to metallic Ni, nickel hydroxide, and shake up satellites, respectively [38,39]. The nickel hydroxide could be attributed to water vapour and O₂ in the air. These XPS results suggest that the electrochemical etching process changed the morphology of SFNi-100, SFNi-150, and SFNi-200 only on the surface, while the chemical properties remained unchanged.

The interface behaviour between the current collector and the electrode material can be expected to play a decisive role in improving the electrochemical performance of supercapacitors. Therefore, in order to better understand the electrochemical behaviour of electrodes, the EIS measurements aiming to explore the charge transfer process were carried out at frequencies ranging from 10⁵ to 10⁻² Hz applying an AC signal of 5 mV. Fig. 4a shows the Nyquist plots of the SFNi-0, SFNi-100, SFNi-150, and SFNi-200 electrodes. In the high-frequency region, the semicircle refers to the charge transfer resistance (R_{ct}) [25,29]. In addition, in the low-frequency region, the slant line denotes the ionic diffusion ability [25,29]. An equivalent circuit was utilized to fit the impedance curve (inset Fig. 4a). Fig. 4b reports the R_{ct} values of the SFNi-0, SFNi-100, SFNi-150, and SFNi-200 electrodes. As can be clearly seen in the results, the R_{ct} of SFNi-150 (0.71 Ω) is considerably smaller than that of SFNi-0 (0.90 Ω), SFNi-100 (0.78 Ω), and SFNi-200 (0.84 Ω), suggesting that the surface functionalization with nano-sized stairs of the terraced surface enhances the electrical contact, leading to an improvement of the charge transfer capability. For that reason, it can be anticipated that, due to the improved charge transfer capability of the SFNi-150 electrode, the nano-sized stairs of terraced surface on the current collector will significantly improve the electrochemical performance during cycling.

To further investigate the effects of interface engineering for supercapacitors, the full-cell system using a commercial activated carbon as a typical active material was prepared in the 6 M KOH electrolytes. Fig. 5a shows the CV curves of the SFNi-0, SFNi-100, SFNi-150, and SFNi-200 electrodes in the potential range of 0.0–1.0 V at the scan rate of 30 mV s⁻¹. All electrodes showed a rectangular curve, implying the ideal occupancy of the electrical double-layer area on the surface of activated carbon used as an active material without redox reaction [31–34]. Fig. 5b shows the CV curves of SFNi-150 at scan rates from 30

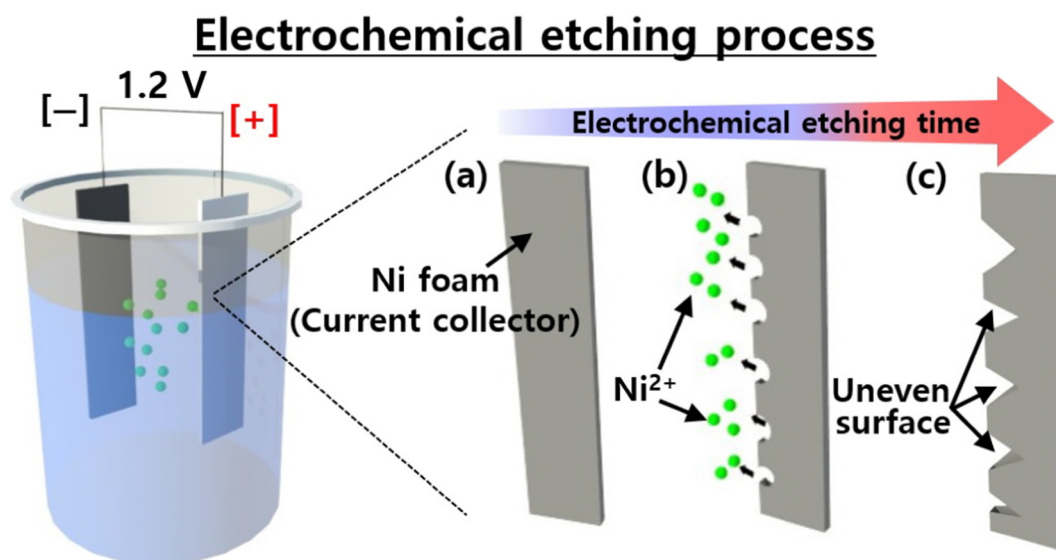


Fig. 1. Schematic illustration of the electrochemical etching process of the Ni foam as the current collector of supercapacitors. (a) Ni foam as the current collector; (b) the dissolution process of Ni^{2+} ; (c) the SFNi with an uneven surface.

to 200 mV s^{-1} in the potential range of 0.0–1.0 V. The rectangular curves maintained their original aspects with an increase of current densities, signifying an ideal electrochemical reaction. In addition, the charge–discharge curves of SFNi-150 at different current densities from 0.5 to 20.0 A g^{-1} are showed in Fig. 5c. The charge–discharge curves at all the current densities indicate nearly symmetric behavior, implying excellent reversibility. The specific capacitance (C_{sp}) (see Fig. 5d) of the SFNi-0, SFNi-100, SFNi-150, and SFNi-200 electrodes was calculated using Eq. (1): [18,20,22].

$$C_{sp} = 4I / (m dV / dt) \quad (1)$$

where I is the current of the charging and discharging processes, m is the mass of the activated carbon as an active material, dV is the voltage drop, and dt is the total time of the discharging process. At the low current density of 0.5 A g^{-1} , the specific capacitances of the SFNi-0, SFNi-100, SFNi-150, and SFNi-200 electrodes amounted to 195, 204, 210, and 201 F g^{-1} , respectively. However, from the results, it is

obvious that, due to the decreased time for the electron transfer, specific capacitances of all electrodes decreased with an increase of current density. The SFNi-0 electrode showed a poor rate performance, indicating that the conventional design of current collectors with a flat surface makes imposes limitations of electron transfer at high rate current densities. Therefore, in order to improve the electron transfer performance, the surface functionalization with nano-sized stairs of the terraced surface was devised. Of note, at the high current density of 20.0 A g^{-1} , the SFNi-150 electrode showed the excellent rate performance of 176 F g^{-1} . Furthermore, the SFNi-150 electrode exhibited the highest capacitance retention (83%) between the current densities from 0.5 to 20.0 A g^{-1} than that of SFNi-0 (60%), SFNi-100 (78%), and SFNi-200 (65%) electrodes. Therefore, the enhanced rate performance of SFNi-150 electrode can mainly be attributed to the improved electron transfer performance of the current collector resulting from the optimization for nano-sized stairs of the terraced surface. Moreover, the cycling stability of electrodes is crucial for the use of supercapacitors in

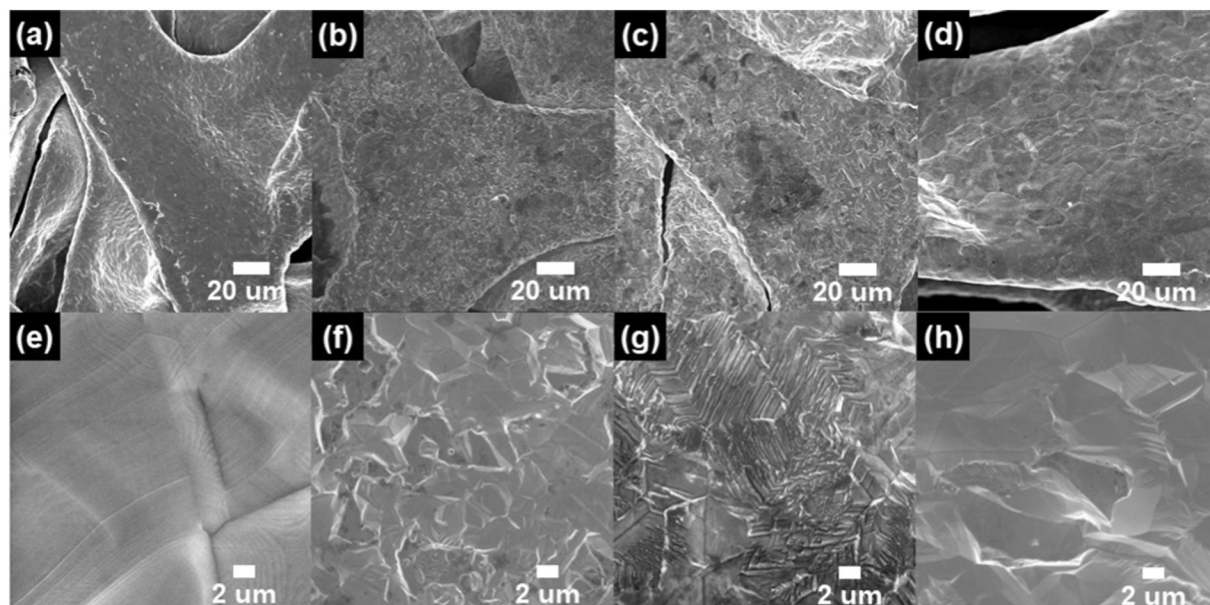


Fig. 2. (a–c) Low-resolution and (d–f) high-resolution SEM images of SFNi-0, SFNi-100, SFNi-150, and SFNi-200.

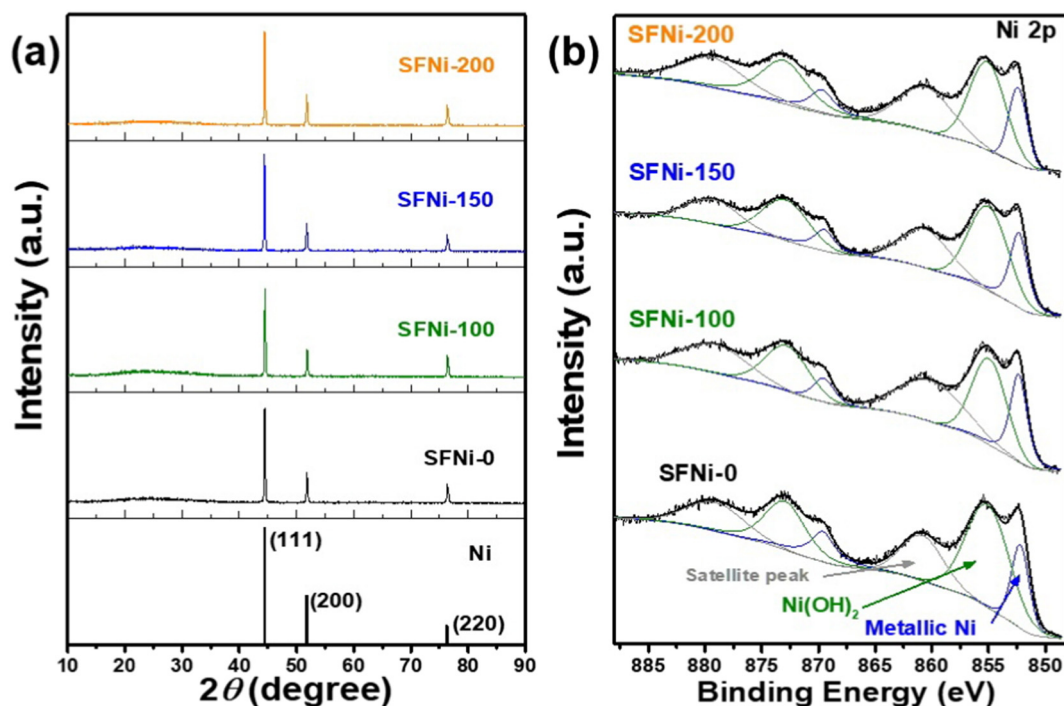


Fig. 3. (a) The XRD patterns and (b) the XPS signals of Ni 2p of SFNi-0, SFNi-100, SFNi-150, and SFNi-200.

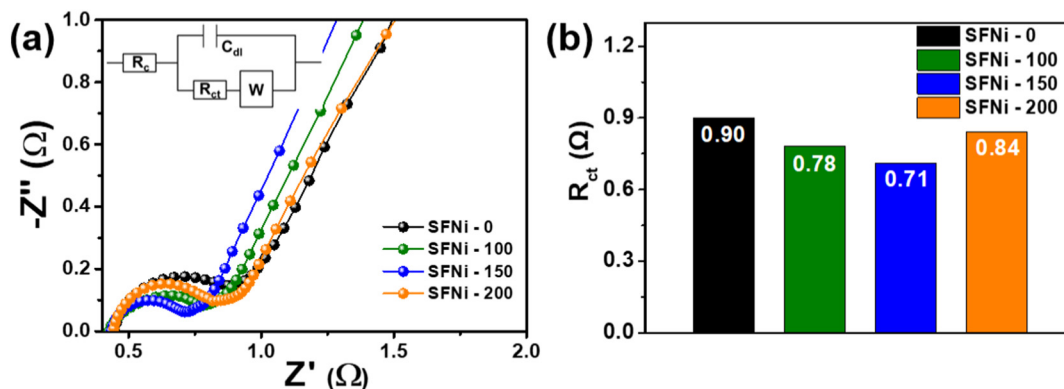


Fig. 4. (a) Nyquist plots in the frequency range of 10^5 – 10^{-2} Hz and (b) the detailed value of R_{ct} for SFNi-0, SFNi-100, SFNi-150, and SFNi-200.

realistic applications. Fig. 5e shows the cycling stability of the SFNi-0, SFNi-100, SFNi-150, and SFNi-200 electrodes at the current density of 5.0 A g^{-1} over 10,000 cycles. In this respect, while the SFNi-150 electrode showed the outstanding capacitance retention of 89%, the SFNi-0, SFNi-100, and SFNi-200 electrodes had the relatively poor capacitance retention of 71, 85, and 79%, respectively. These results suggest that the electrochemical etching process of the current collector was optimised using 150 s. Therefore, nano-sized stairs of SFNi-150 electrode could provide a strong interfacial adhesion between the current collector and electrode material, leading to an improvement of cycling stability. However, SFNi-0, SFNi-100, and SFNi-200 electrodes indicated the relatively poor cycling stability compared to SFNi-150 electrode due to the flat surface without nano-sized stairs on the surface.

In their entirety, the results of the present suggest that the strikingly improved energy storage performance of the SFNi-150 electrode may be attributed to the establishing a novel surface functionalization of the current collector having nano-sized stairs of the terraced surface (see Fig. 6). The high contact area between the current collector and the electrode material provides an enhanced charge transfer capability, which leads to the outstanding rate performance. In addition, the

uneven surface creates a strong interfacial adhesion between the current collector and the electrode material, leading an enhanced cycling stability.

4. Conclusions

In the present study, we have proposed an innovative interface engineering concept of the interface between the current collector and electrode material of supercapacitors. The proposed interface design is based on surface functionalization of the Ni foam as the current terrace surface-based collector with nano-sized stairs. As demonstrated by specific capacitance (210 F g^{-1} at the current density of 0.5 A g^{-1}), a remarkable rate performance of 83%, and an impressive cycling stability of 89% after 10,000 cycles, the improved energy storage performance of the SFNi-150 electrode was achieved. The high contact area between the current collector and the electrode material facilitates enhancing the rate performance, enabling thus a superior charge transfer capability. Furthermore, the uneven surface was used to enhance the cycling stability using the strong interfacial adhesion between the current collector and the electrode material. Therefore, the novel surface design of the current collector is a new approach

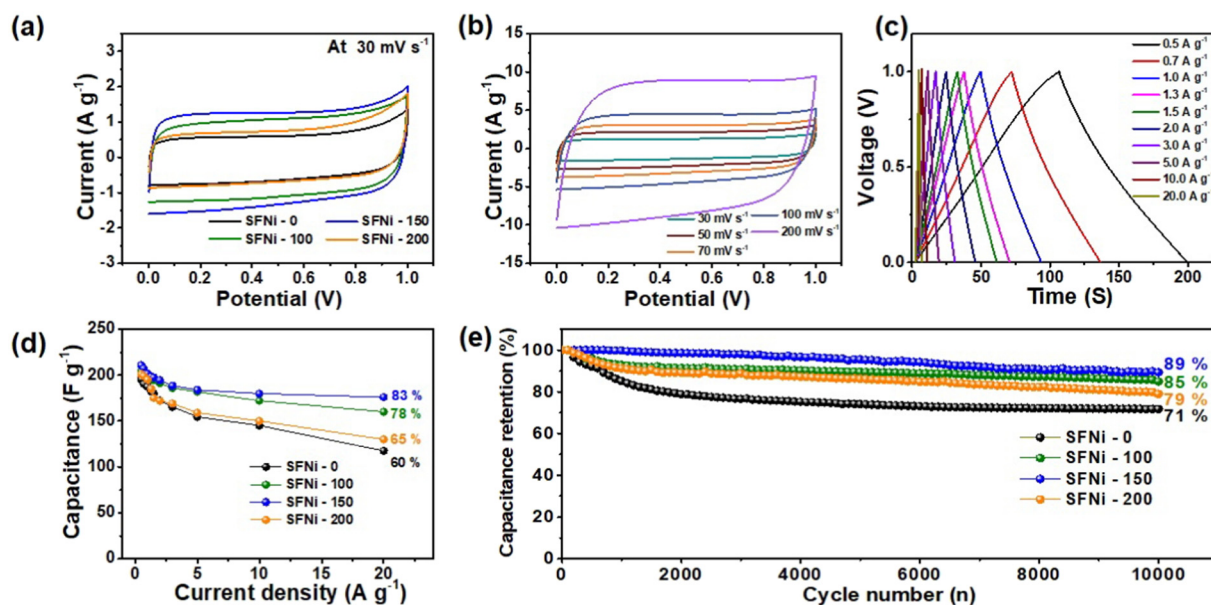


Fig. 5. (a) the CV curves at the scan rate of 30 mV s^{-1} in the potential range 0.0 to 1.0 V; (b) the CV curves of SFNi-150 at scan rates varying from 30 to 200 mV s^{-1} in the potential range 0.0 to 1.0 V; (c) Galvanostatic charge–discharge curves of SFNi-150 at current densities from 0.5 to 20.0 A g^{-1} in the potential range 0.0 to 1.0 V; (d) the calculated specific capacitances at current densities in the range $0.5\text{--}20.0 \text{ A g}^{-1}$; (e) the cycling stability at the current density of 5 A g^{-1} over 10,000 cycles.

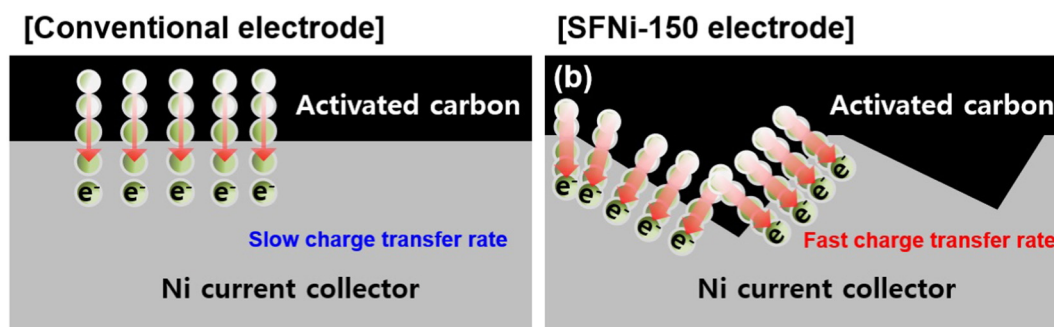


Fig. 6. Comparison of the conventional and the proposed designs of the SFNi-150 electrode during the charge transfer of supercapacitors.

meaningful not only for fundamental research in interface engineering, but also for the applied tasks, such as enhancing the charge transfer capability for supercapacitors.

Acknowledgments

This study was supported by the Advanced Research Project funded by the SeoulTech (Seoul National University of Science and Technology).

References

- [1] C. Li, J. Balamurugan, N.H. Kim, J.H. Lee, *Adv. Energy Mater.* 8 (2018) 1702014.
- [2] P. Simon, Y. Gogotsi, *Nat. Mater.* 7 (2008) 845–854.
- [3] G. Wang, L. Zhang, J. Zhang, *Chem. Soc. Rev.* 41 (2012) 797–828.
- [4] P. Simon, Y. Gogotsi, B. Dunn, *Science* 343 (2014) 1210–1211.
- [5] L.-Q. Fan, G.-J. Liu, C.-Y. Zhang, J.-H. Wu, Y.-L. Wei, *Int. J. Hydrog. Energy* 40 (2015) 10150–10157.
- [6] G.-H. An, H.-J. Ahn, *Appl. Surf. Sci.* 473 (2019) 77–82.
- [7] L. Shen, L. Du, S. Tan, Z. Zang, C. Zhao, W. Ma, *Chem. Commun.* 52 (2016) 6296–6299.
- [8] G.-H. An, D.-Y. Lee, H.-J. Ahn, *J. Ind. Eng. Chem.* 65 (2018) 423–428.
- [9] W. Chen, C. Xia, H.N. Alshareef, *ACS Nano* 8 (2014) 9531–9541.
- [10] G.-H. An, S.N. Cha, J.I. Sohn, *Appl. Surf. Sci.* 467–468 (2019) 1157–1160.
- [11] S. Zhu, L. Li, J. Liu, H. Wang, T. Wang, Y. Zhang, L. Zhang, R.S. Ruoff, F. Dong, *ACS Nano* 12 (2018) 1033–1042.
- [12] C. Jing, X. Liu, X. Liu, D. Jiang, B. Dong, F. Dong, J. Wang, N. Li, T. Lane, Y. Zhang, *CrystEngComm* 20 (2018) 7428–7434.
- [13] X. Guo, T. Zheng, G. Ji, N. Hu, C. Xu, Y. Zhang, *J. Mater. Chem. A* 6 (2018) 10243–10252.
- [14] H. Chen, X.L. Liu, J.M. Zhang, F. Dong, Y.X. Zhang, *Ceram. Int.* 42 (2016) 8909–8914.
- [15] G.-H. An, D.-Y. Lee, H.-J. Ahn, *J. Mater. Chem.* 5 (2017) 19714–19720.
- [16] Y. Liu, Z. Zhou, S. Zhang, W. Luo, G. Zhang, *Appl. Surf. Sci.* 442 (2018) 711–719.
- [17] Y. Cheng, B. Li, Y. Huang, Y. Wang, J. Chen, D. Wei, Y. Feng, D. Jia, Y. Zhou, *Appl. Surf. Sci.* 439 (2018) 712–723.
- [18] D.-Y. Lee, G.-H. An, H.-J. Ahn, *J. Ind. Eng. Chem.* 52 (2017) 121–127.
- [19] D. Qu, X. Feng, X. Wei, L. Guo, H. Cai, H. Tang, Z. Xie, *Appl. Surf. Sci.* 413 (2017) 344–350.
- [20] G.-H. An, H.-J. Ahn, *Carbon* 65 (2013) 87–96.
- [21] C. Cai, Y. Zou, C. Xiang, H. Chu, S. Qiu, Q. Sui, F. Xu, L. Sun, A. Shah, *Appl. Surf. Sci.* 440 (2018) 47–54.
- [22] G.-H. An, B.-R. Koo, H.-J. Ahn, *Phys. Chem. Chem. Phys.* 18 (2016) 6587–6594.
- [23] Q. Xie, X. Huang, Y. Zhang, S. Wu, P. Zhao, *Appl. Surf. Sci.* 443 (2018) 412–420.
- [24] X. Xu, J. Gao, Q. Tian, X. Zhai, Y. Liu, *Appl. Surf. Sci.* 411 (2017) 170–176.
- [25] Y.-W. Lee, G.-H. An, B.-S. Kim, J. Hong, S. Pak, E.-H. Lee, Y. Cho, J. Lee, P. Giraud, S.N. Cha, H.-J. Ahn, J.I. Sohn, J.M. Kim, *ACS Appl. Mater. Interfaces* 8 (2016) 17651–17658.
- [26] X.-L. Su, J.-R. Chen, G.-P. Zheng, J.-H. Yang, X.-X. Guan, P. Liu, X.-C. Zheng, *Appl. Surf. Sci.* 436 (2018) 327–336.
- [27] A.A. Silva, R.A. Pinheiro, A.C. Rodrigues, M.R. Baldan, V.J. Trava-Airoldi, E.J. Corat, *Appl. Surf. Sci.* 446 (2018) 201–208.
- [28] G.-H. An, H. Kim, H.-J. Ahn, *ACS Appl. Mater. Interfaces* 10 (2018) 6235–6244.
- [29] G.-H. An, D.-Y. Lee, H.-J. Ahn, *ACS Appl. Mater. Interfaces* 9 (2017) 12478–12485.
- [30] M. Guo, Y. Li, K. Du, C. Qiu, G. Dou, G. Zhang, *Appl. Surf. Sci.* 440 (2018) 606–613.
- [31] Z. Xu, Y. Li, D. Li, D. Wang, J. Zhao, Z. Wang, M.N. Banis, Y. Hu, H. Zhang, *Appl. Surf. Sci.* 444 (2018) 661–671.
- [32] K. Wu, Q. Liu, *Appl. Surf. Sci.* 379 (2016) 132–139.
- [33] J. Liang, T. Qu, X. Kun, Y. Zhang, S. Chen, Y.-C. Cao, M. Xie, X. Guo, *Appl. Surf. Sci.* 436 (2018) 934–940.
- [34] L. Pan, X. Li, Y. Wang, J. Liu, W. Tian, H. Ning, M. Wu, *Appl. Surf. Sci.* 444 (2018) 739–746.

- [35] M.M. Rieger, P.A. Kohl, *J. Electrochem. Soc.* 142 (1995) 1490–1495.
- [36] J.H. Seo, J.-H. Ryu, D.N. Lee, *J. Electrochem. Soc.* 150 (2003) B433–B438.
- [37] G.-H. An, H.-G. Jo, H.-J. Ahn, *J. Alloys Compd.* 763 (2018) 250–256.
- [38] S.H. Gage, C. Ngo, V. Molinari, M. Causà, R.M. Richards, F.S. Gentile, S. Pylypenko, D. Esposito, *J. Phys. Chem. C* 122 (2018) 339–348.
- [39] M.K. Jeon, K.R. Lee, H.J. Jeon, P.J. McGinn, K.H. Kang, G.I. Park, *Korean J. Chem. Eng.* 32 (2015) 206–215.